

Cluster–oxalate frameworks with extra-large channels: solvent-free synthesis, chemical stability, and proton conduction

Lindong Luan,^{a,b} Ying Zhang,^a Hongmei Zeng,^a Guohong Zou,^a Yong Dai,^b Xiaoying Zhou^{*b} and Zhien Lin^{*}

^a *College of Chemistry, Sichuan University, Chengdu 610064, P. R. China.*

^b *Department of Criminal Science and Technology, Sichuan Police College, Luzhou 646000, P. R. China*

* To whom correspondence should be addressed. Tel: +86-28-85412284. E-mail: 907287136@qq.com (X. Zhou); zhienlin@scu.edu.cn (Z. Lin)

Physical measurements:

Powder X-ray diffraction (XRD) data were obtained using a Rigaku D/MAX-rA diffractometer with Cu-K α radiation ($\lambda = 1.5418 \text{ \AA}$). IR spectra (KBr pellets) were recorded on a Nicolet Impact 410 FTIR spectrometer. The thermogravimetric analyses were performed on a Netzsch STA 449c analyzer in a flow of N₂ with a heating rate of 10 °C/min. Magnetic measurement was performed on the Quantum Design SQUID MPMS XL-7 magnetometer in a magnetic field of 1000 Oe in the temperature range of 2-300 K. Alternating current impedance measurements were carried out with a Solartron SI 1260 impedance/gain-phase analyzer over the frequency range from 0.1 Hz to 10 MHz with an applied voltage of 10 mV. The relative humidity was controlled by a STIK Corp. CIHI-150B incubator. The sample was pressed to form a cylindrical pellet of crystalline powder sample (~2 mm thickness \times 5 mm ϕ) coated with C-pressed electrodes. Two silver electrodes were attached to both sides of pellet to form four end terminals (quasi-four-probe method). Single crystal X-ray diffraction data were collected on a New Gemini, Dual, Cu at zero, EosS2 diffractometer at room temperature. The crystal structures were solved by direct methods. The structures were refined on F^2 by full-matrix least-squares methods using the *SHELXTL* program package.¹

Reference

1. G. M. Sheldrick, *Acta Cryst., Sect. A*, 2008, 64, 112.

Table S1. Hydrogen bond information for SCU-62

| D-H...A ^a | d(D-H) (Å) | d(H...A) (Å) | d(D...A) (Å) | <(DHA) (deg) |
|----------------------|------------|--------------|--------------|--------------|
| N1-H1...O8#1 | 0.86 | 1.87 | 2.672(6) | 154.8 |
| N1-H2...O2#2 | 0.86 | 2.21 | 2.882(7) | 135.4 |

^aSymmetry transformations used to generate equivalent atoms: #1 1-x, 1-y, +z; #2 1/2+y, 1-x, -1/4+z.

Table S2. Hydrogen bond information for SCU-65

| D-H...A ^a | d(D-H) (Å) | d(H...A) (Å) | d(D...A) (Å) | <(DHA) (deg) |
|----------------------|------------|--------------|--------------|--------------|
| N1-H1...O6#1 | 0.98 | 2.09 | 2.997(4) | 152.8 |
| N2-H2A...O10 | 0.89 | 2.45 | 3.233(4) | 147.2 |
| N2-H2B...O6#1 | 0.89 | 1.99 | 2.828(4) | 157.5 |
| N2-H2C...O1 | 0.89 | 2.34 | 2.882(4) | 119.1 |
| N2-H2C...O2 | 0.89 | 2.27 | 3.143(4) | 165.3 |

^aSymmetry transformations used to generate equivalent atoms: #1 2-x, 1-y, 1-z.

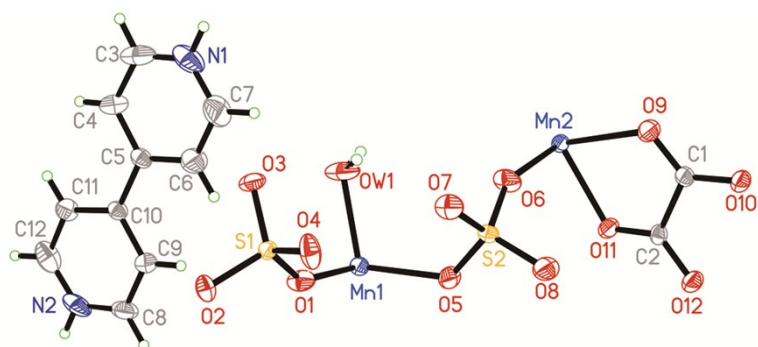


Fig. S1. ORTEP plot of the asymmetric unit of SCU-62, showing the labeling scheme and the 50% probability displacement ellipsoid.

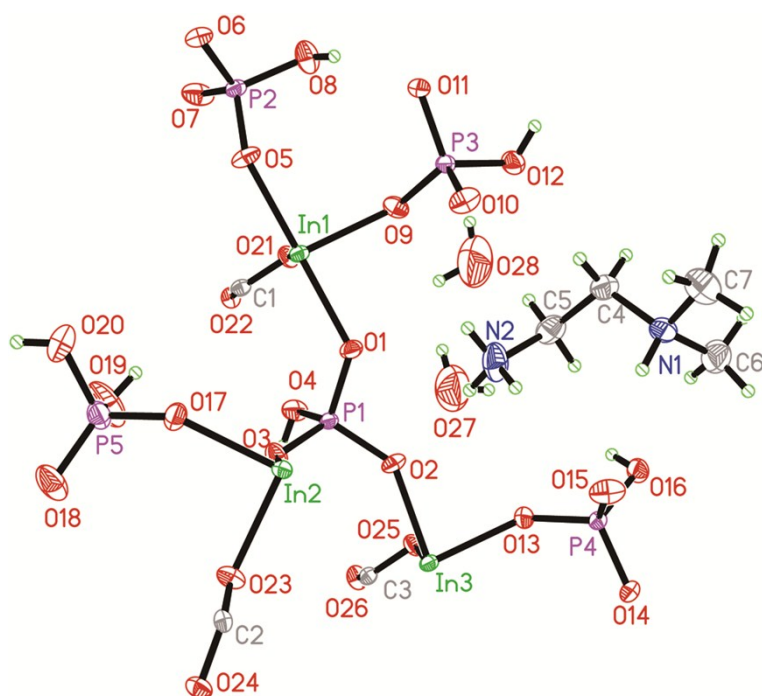


Fig. S2. ORTEP plot of the asymmetric unit of SCU-65, showing the labeling scheme and the 50% probability displacement ellipsoid.

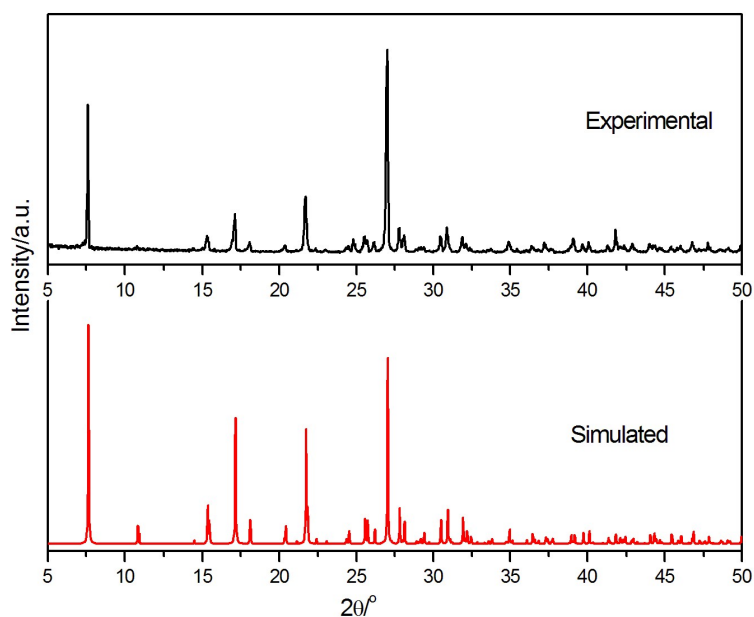


Fig. S3. Experimental and simulated powder XRD patterns of SCU-62.

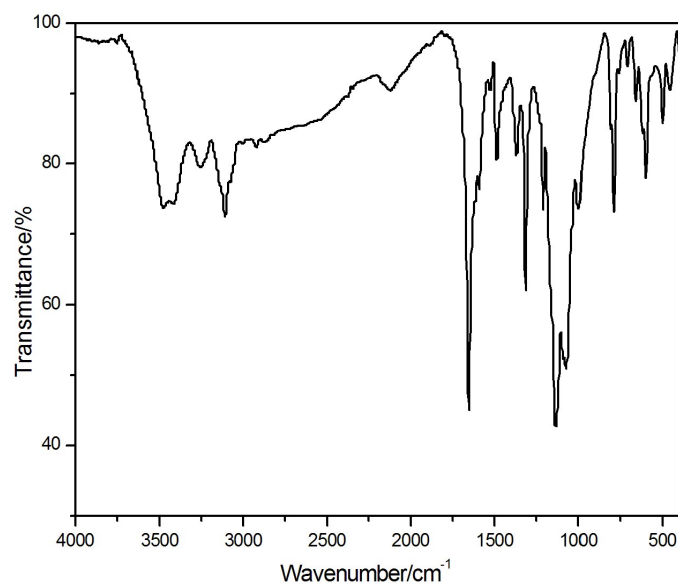


Fig. S4. IR spectrum of SCU-62. The strong bands at 1650 and 1320 cm^{-1} correspond to the C=O and C–O stretching vibrations in the oxalate groups, respectively. The strong bands in the region 995–1140 cm^{-1} are assigned to the asymmetric stretch of SO_4 tetrahedra. The weak bands for CH_2 bending vibration appear at 1485 cm^{-1} . The band at 1370 cm^{-1} is assigned to the C–N stretching vibration.

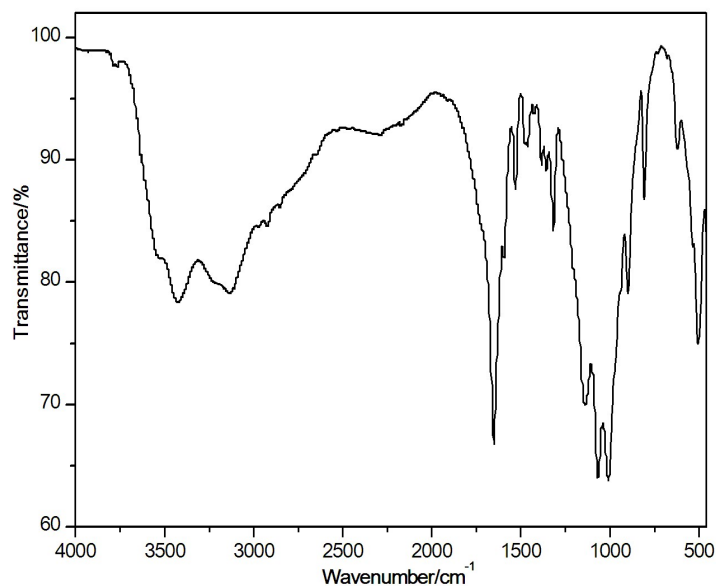


Fig. S5. IR spectrum of SCU-65. The bands at 1652 and 1316 cm^{-1} correspond to the C=O and C-O stretching vibrations in the oxalate groups, respectively. The strong bands in the region 1000-1150 cm^{-1} are assigned to the asymmetric stretch of PO_4 tetrahedra. Also present are the weak bands for CH_2 bending vibration at 1465 cm^{-1} , and a C-N stretching band at 1380 cm^{-1} .

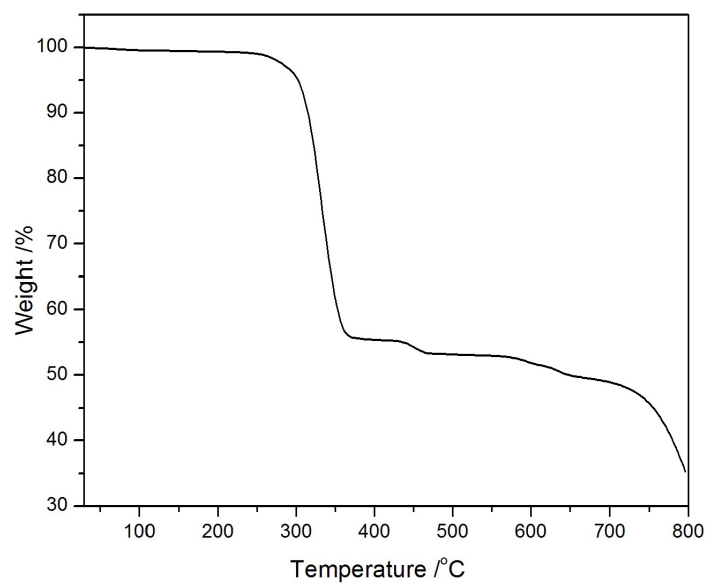


Fig. S6. TGA curve of SCU-62.

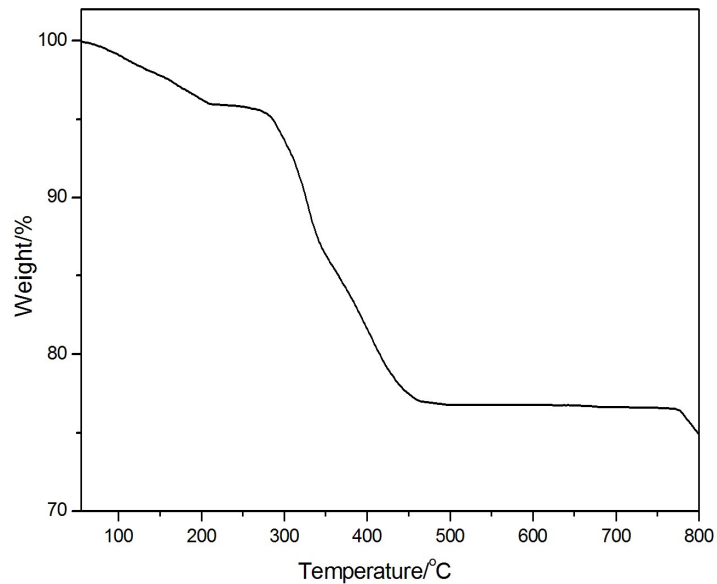


Fig. S7. TGA curve of SCU-65.

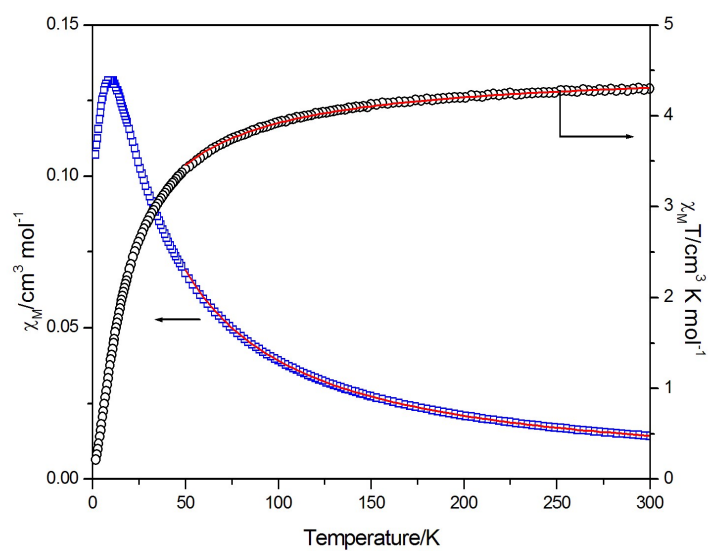


Fig. S8. Temperature dependence of χ_M and $\chi_M T$ for SCU-62. The solid lines are fit to the Curie-Weiss law in the high-temperature region.

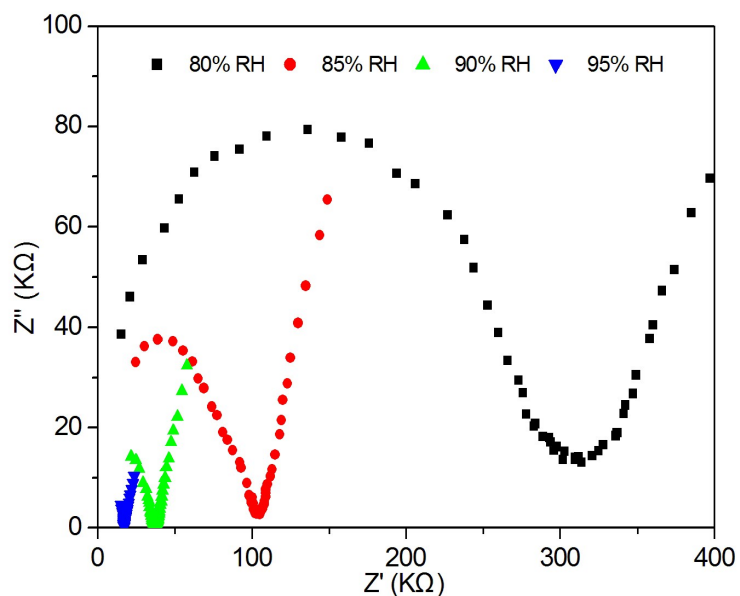


Fig. S9. Nyquist plots for SCU-65 at 85 °C under different RH conditions. The conductivity is $3.0 \times 10^{-6} \text{ S}\cdot\text{cm}^{-1}$ (80% RH), $9.0 \times 10^{-6} \text{ S}\cdot\text{cm}^{-1}$ (85% RH), $2.5 \times 10^{-5} \text{ S}\cdot\text{cm}^{-1}$ (90% RH), and $5.5 \times 10^{-5} \text{ S}\cdot\text{cm}^{-1}$ (95% RH).

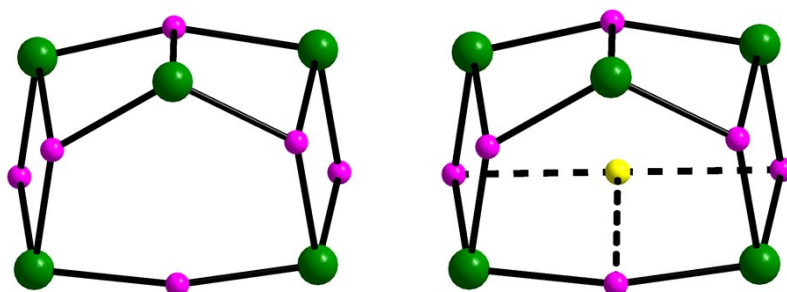


Fig. S10. (left) Topological representation of the lacunary D6R cluster. (right) The lacunary D6R cluster can be converted into a regular D6R unit by inserting a node at the crystallographic site position (1.0387, 1.6997, 2.3053).